APPLIED ORGANOMETALLIC CHEMISTRY
Appl. Organometal. Chem. 2004; **18**: 205–211
Published online in Wiley InterScience (www.interscience.wiley.com). DOI:10.1002/aoc.602

UV photosynthesis of nickel carbonyl

Xuming Guo, Ralph E. Sturgeon*, Zoltan Mester and Graeme Gardner

Institute for National Measurement Standards, National Research Council of Canada, Ottawa, Ontario K1A 0R9, Canada

Received 23 July 2003; Revised 20 October 2003; Accepted 18 December 2003

In the presence of low-molecular-weight organic acids, such as formic, acetic, and propionic, inorganic nickel salts in aqueous solutions are converted to the volatile tetracarbonyl by UV irradiation. Experiments were performed using a flow-through photoreactor, consisting of a 6 m length polytetrafluoroethylene tubing wrapped around a low-pressure mercury vapor UV lamp (254 nm, 15 W). The efficiency of transformation was estimated to be 95%. As no carbon monoxide or external reductant is required, photochemical synthesis may prove to be useful in material chemistry and applicable to the extractive metallurgy of nickel, as well as its refining and recycling. Copyright © 2004 Crown in the right of Canada. Published by John Wiley & Sons, Ltd.

KEYWORDS: nickel; carbonyl; photolysis; UV

INTRODUCTION

In 1879, Mond discovered that carbon monoxide, passed over finely divided nickel metal, formed gaseous nickel tetracarbonyl ($Ni(CO)_4$). This is a readily reversible reaction, in that the carbonyl can be decomposed to yield nickel metal and carbon monoxide at 180 °C.[1] The resulting Mond process became one of the truly elegant metallurgical procedures, and the discovery was also a notable step in the history of organometallic chemistry, which led to Reppe catalysts (using nickel carbonyl for synthesis). Nickel catalyzes the gasification of biomass and is also operative in biological systems,[2–7] catalyzing biochemical reactions. The discovery of new synthetic methods for production of nickel carbonyl and its cluster species is of interest not only for application to new commercial materials, but also because of its theoretical significance, for it enriches our information of metal cluster bonding, permitting further insight into an understanding of chemical reactions under various conditions.

Methods for the production of $Ni(CO)_4$ have been documented in 55 patents since 1955,[8] most of them dealing with dry contact methods for the reduction of ores, oxides, or salts for preparing the highly active metal, followed by reaction with carbon monoxide (CO). The discovery of new and easier preparative procedures for organometallic compounds has always been regarded as a great rebirth or expansion of classical organometallic chemistry.[9]

In previous work,[10,11] we have reported that inorganic selenium(IV) in aqueous media can be converted to volatile selenium carbonyl (SeCO), dimethylselenide ($(CH_3)_2Se$) and diethylselenide ($(CH_3CH_2)_2Se$) in the presence of formic (HCOOH), acetic (CH_3COOH), propionic (CH_3CH_2COOH) and/or malonic acids when subjected to UV irradiation. We report here on studies showing that Ni^{2+} can be converted to $Ni(CO)_4$ in similar media without intervention by CO or addition of reducing agents.

EXPERIMENTAL

A flow-through photoreactor was constructed, consisting of a 6 m length of 1.1 mm i.d. × 1.7 mm o.d. polytetrafluoroethylene (PTFE) tubing (Cole Parmer Instrum. Co., Vernon Hills, IL) wrapped around a low-pressure mercury vapor UV lamp (254 nm, 15 W; Cole Parmer, USA). A schematic of this system is illustrated in Fig. 1. Samples were propelled through the tubing with the aid of a Minipuls 2 peristaltic pump (Gilson, Middleton, WI) operating at a speed of 50 rev min^{-1}, corresponding to a solution flow rate of 2 ml min^{-1} and solution irradiation times of 4 min. UV vapor generation was accomplished in a continuous-flow mode as the sample was passed through the PTFE tube for irradiation. A 55 ml min^{-1} flow of helium purge gas was introduced into a gas–liquid separator, where the effluent from the UV photoreactor was merged directly with the helium flow. The resultant volatile species were transported by the helium flow from the gas–liquid separator either directly to an air–acetylene flame via a 10 cm

*Correspondence to: Ralph E. Sturgeon, Institute for National Measurement Standards, National Research Council of Canada, Ottawa, Ontario K1A 0R9, Canada.
E-mail: ralph.sturgeon@nrc.ca

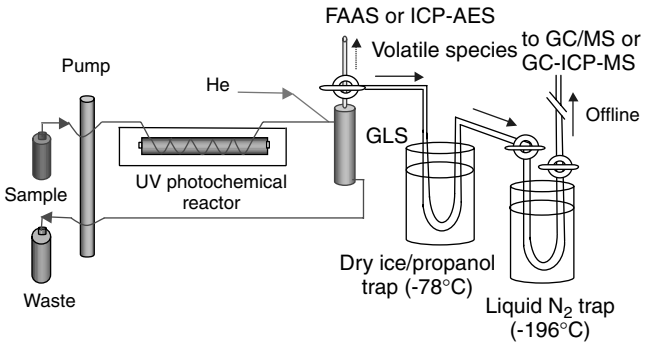

Figure 1. Schematic of the experimental system.

length of PTFE transfer tubing for detection by atomic absorption spectrometry, or through an intermediate cryogenically cooled U-shaped glass condensation tube for collection and subsequent characterization.

A Perkin–Elmer Model Analyst 100 flame atomic absorption spectrometer (F-AAS) fitted with flame atomizer and a Perkin–Elmer hollow-cathode nickel lamp was operated under the following conditions: wavelength, 232.0 nm; slit setting, 0.2 nm; current, 18 mA; acetylene flow rate, 3 l min^{-1}; air flow rate, 10 l min^{-1}. Simultaneous deuterium background correction was applied to all measurements. Both peak height and integrated absorbance measurements were recorded. An IRIS inductively coupled plasma (ICP) optical emission spectrometer (OES; Thermo Jarrell Ash Co.) was employed to confirm all results obtained with the F-AAS, as it offers improved detection limits. Relevant plasma and detection operating parameters are as follows: RF power 1150 W; outer argon gas flow rate, 14 l min^{-1}; intermediate argon gas flow rate 0.8 l min^{-1}; argon carrier gas flow rate, 0.38 l min^{-1}; nickel wavelength, 231.6 nm.

Measurements were made in a continuous on-line mode to characterize the yield of the reaction products and also in an off-line manner to trap the volatile species in an effort to subsequently characterize them via gas chromatography (GC) coupled with mass spectrometry (MS) and GC–ICP-MS techniques. For this latter purpose, a series of cryogenically cooled Pyrex U-tube traps (0.8 cm o.d. × 0.6 cm i.d. × 13 cm deep × 4 cm across) were occasionally placed between the generator and the detector to condense the generated analyte species, as described below.

In order to avoid clogging of the cryogenically cooled Pyrex U-tube and possible decomposition of any volatile nickel compounds by concomitant water, a dry-ice–methanol trap (−78 °C) was used, into which a 'guard' Pyrex U-tube (1.7 cm o.d. × 1.5 cm i.d. × 13 cm deep × 6 cm across) was immersed to remove any water vapor carried over from the UV photochemical reaction system. Following completion of the reaction, the dry-ice–methanol bath was removed from the first U-tube; this tube was then maintained at ambient temperature for 5 min, such that any collected volatile nickel compounds could be transferred to the second U-tube where they were re-deposited under liquid-nitrogen bath temperatures. The second U-tube, packed with glass wool and immersed in liquid nitrogen (−196 °C), was thus used for trapping the volatile species swept from the dry-ice bath. Continuous on-line monitoring of the AAS signal revealed that the volatile nickel species were completely trapped in this second U-tube. High-purity helium was chosen as the carrier gas as it is not condensed in the U-tube at liquid-nitrogen temperatures and does not introduce any mass spectral interference during the subsequent identification of trapped species using GC–ICP-MS and GC–MS. Prior to commencing the trapping experiment, the U-tubes were flushed with helium for 10 min at room temperature.

A Hewlett-Packard (HP) model 6890 gas chromatograph was interfaced to an HP 5973 mass-selective detector (mass range monitored 60–270 Da). Nickel compounds were separated on a 30 m × 0.25 mm i.d. × 0.25 mm film (J&W Scientific) DB1 capillary column (1% phenyl, 99% polydimethylsiloxane) using UHP helium carrier gas and a head pressure of 12.5 psi. Splitless sample injection was used. Sample aliquots of 250 µl were manually injected. The transfer-line temperature was 40 °C. The carrier gas flow rate was set at 1.2 ml min^{-1}. An 18 min temperature program was used with an initial temperature of 30 °C and a hold time of 10 min, followed by a ramp of 60 °C min^{-1} to a temperature of 280 °C, which was held for 10 min.

A Perkin–Elmer SCIEX ELAN 6000 (Concord, Ontario, Canada) ICP-MS instrument was interfaced to a Varian 3400 GC (Varian Canada, Georgetown, Canada) equipped with a 15 m length of DB-1 column (0.32 mm) through an in-house heated transfer line. The sampling process and GC conditions were similar to those used above for GC–MS measurements. The ICP-MS instrument was operated in accordance with the manufacturer's recommendations, with the ^{60}Ni and ^{61}Ni isotopes selected rather than using the more abundant ^{58}Ni for detection in order to eliminate possible isobaric inferences arising from ArO^+.

Reagents and samples

All solutions were prepared using 18 MΩ cm deionized, reverse osmosis water (DIW) obtained from a mixed-bed ion-exchange system (NanoPure, model D4744, Barnstead/Thermoline, Dubuque, IA). Calibration solutions were prepared daily by diluting the stock solutions. Nickel stock solutions (1000 mg l^{-1}) were prepared from $NiCl_2$, $NiSO_4$, and $Ni(NO_3)_2$ (Aldrich, USA). Solutions of low-molecular-weight (LMW) acids were prepared from analytical reagent-grade materials: HCOOH (23 M, Anachemica, Canada), acetic acid (6.3 M, BDH, Canada) and propionic acid (13 M, BDH). All gases (argon and helium) were of high purity and obtained from Praxair Products Inc. (Mississauga, ON, Canada).

Procedure

Volatile nickel compounds were generated when the nickel standard solutions containing various LMW acids at different

concentrations were pumped through the PTFE tubing of the photoreactor. The gaseous products were separated from the liquid phase in the gas–liquid separator and flushed into the air–acetylene flame for AAS detection, ICP-OES detection, or passed through the successive U-tubes using a stream of helium carrier gas. For the latter approach, following cryocondensation, the second U-tube was closed at both ends by rubber septa, removed from the liquid-nitrogen bath and allowed to equilibrate to room temperature for about 15 min. A 250 μl volume of the gas phase containing the volatile nickel species was sampled through the septum of the U-tube using a gas-tight syringe and injected into the chromatograph for species identification by GC–MS.

Safety considerations

Some volatile nickel compounds are toxic, and contact with $Ni(CO)_4$ is dangerous. The full range of such compounds produced in these studies may not be known. Essential safety precautions must be taken during all manipulations and an adequate ventilation/exhaust system used.

RESULTS AND DISCUSSION

Effects of generation medium

Volatile nickel species were rapidly formed in the photoreactor, giving rise to relatively sharp atomic absorption signals in a matter of only a few minutes. HCOOH was initially investigated for its effects on the generation of volatile nickel species, as it has the simplest structure among the organic acids studied. Short irradiation times (4 min) in the presence of HCOOH resulted in the AAS detection of signals whose intensities were strongly dependent on the acidity of the reaction medium, as shown by the data in Fig. 2. No plateau in the range of 2–23.0 M HCOOH is evident, suggesting that the optimum acidity range lies at yet higher concentrations of HCOOH, if these could be accessed. This is evident from the substantial increase in response obtained by the addition of formate ion to the concentrated HCOOH (23 M). Enhanced detection power was achieved using an ICP-OES. Results are presented in Fig. 3. Additional studies revealed that the plateau for optimum acidity and formate ion concentration can be obtained in the presence of 23 M HCOOH together with 1–3.0 M HCOONa. It is noteworthy that volatile nickel species are also generated from solutions containing formate anions alone; however, the generation efficiency appears to be significantly lower when compared with that in the HCOOH system (see Fig. 3). Efforts aimed at decreasing the concentration of HCOOH based on the addition of formate anion appear not to be successful, suggesting that use of HCOOH concentrations as high as possible (i.e. 23 M) are necessary. This can be clearly seen from the data in Fig. 4. In order to distinguish further the role played by formate anion ($HCOO^-$) in enhancing signal intensity, as opposed to a simple increase in solution pH, a series of acetate (CH_3COONa) or NaOH solutions were substituted for $HCOO^-$. Both acetate and NaOH, when added to the 23 M HCOOH, resulted in the same intensity enhancement effects on the nickel signal as those produced by the sodium formate. Clearly, this positive effect does not simply arise from the increased formate anion concentration, considering that the addition of less than 3 M formate to the 23 M formic acid solution only slightly changes the pH. It might thus be speculated that production of the volatile nickel species is favored by a buffered system in which the pH is stable before and after the photochemical reaction. In this work, 23 M formic acid plus 0.5 M sodium formate was selected as the optimum reaction medium, along with an irradiation time of 4 min.

Apart from HCOOH, CH_3COOH can also be used to generate volatile nickel compounds under UV irradiation. The effects of acid concentration on the intensity of the AAS signal for a solution containing 10 mg l^{-1} Ni^{2+} are shown in Fig. 2. With increasing concentration of acetate anion, the nickel signal intensity increases. Furthermore, enhancement

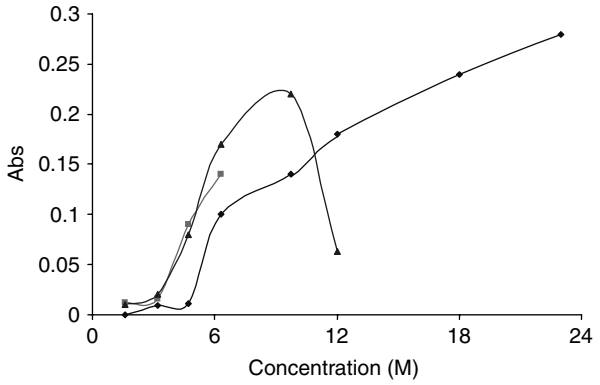

Figure 2. Effect of concentration of LMW organic acids on the F-AAS signals arising from the continuous photochemical irradiation of solutions containing 10 mg l^{-1} Ni^{2+}: ♦ HCOOH; ■ CH_3COOH; ▲ CH_3CH_2COOH.

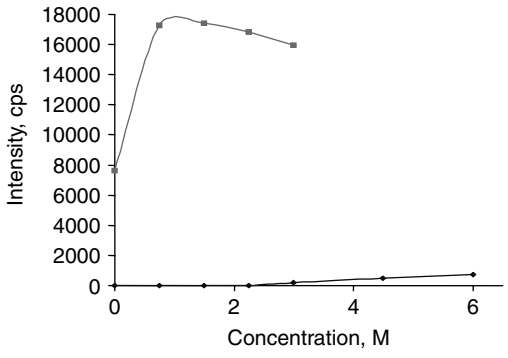

Figure 3. Effect of concentration of $HCOO^-$ ions on ICP-OES response arising from the continuous photochemical irradiation of solutions containing 0.5 mg l^{-1} Ni^{2+}: ♦ $HCOO^-$ only; ■ $HCOO^-$ + 23M HCOOH.

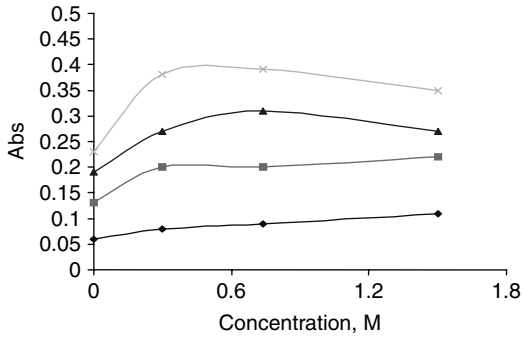

Figure 4. Effect of concentration of $HCOO^-$ ions in the presence of various concentrations of HCOOH on the F-AAS signals arising from the continuous photochemical irradiation of solutions containing 20 mg l^{-1} Ni^{2+}: ♦ 6 M; ■ 12 M; ▲ 18 M; ×23 M.

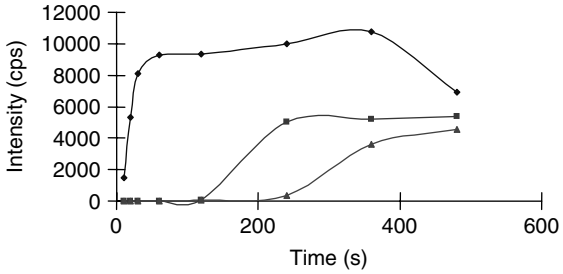

Figure 5. Effect of irradiation time on the F-AAS signals arising from the continuous photochemical irradiation of solutions containing 5 mg l^{-1} Ni^{2+} in the presence of: ♦ 23 M HCOOH + 0.5 M HCOONa; ■ 6.3 M CH_3COOH; ▲ 12 M CH_3CH_2COOH.

effects noted earlier following the addition of sodium, sodium acetate, or OH^- anions no longer occur.

A different situation was obtained when CH_3CH_2COOH was used in the reaction medium (see Fig. 2), as a sharp peak in optimum response arises with increasing acid concentration. Volatile nickel species become more difficult to generate when the acid concentration is higher than 10 M. Although the mechanism of action is unclear, an insufficient irradiation time (4 min only) appears to be partially responsible for this decrease, and this point will be discussed later. It is expected that the optimum concentration of CH_3CH_2COOH may be shifted to higher values (up to 8 M) by utilizing an increased irradiation time.

Standards prepared from different compounds of nickel, i.e. $NiCl_2$, $NiSO_4$, and $Ni(NO_3)_2$, were tested in the presence of the various LWM acids; no difference in intensity of the nickel signal was evident. Moreover, $Ni(CO)_4$ is being formed independently of the counter anion of the nickel salt (i.e. Cl^-, SO_4^{2-}, etc.)

Irradiation time

By fixing the sample flow rate and changing the length of the PTFE tube wrapped around the UV lamp, the effect of residence time (irradiation time) of the analyte in the irradiation field could be investigated. For this purpose, a solution containing 5 mg l^{-1} of Ni^{2+} and 23 M HCOOH + 0.5 M HCOONa, or 6.3 M of CH_3COOH, or 12 M CH_3CH_2COOH was used. The results are shown in Fig. 5, wherein it is evident that the optimum irradiation time is different for each of the acids. Acids having longer carbon chains require longer irradiation times. For example, when HCOOH is used, the optimum irradiation time ranges from 50 s to 6 min, whereas at least 4 min is needed when using CH_3COOH, and more than 8 min (likely still insufficient) is needed for CH_3CH_2COOH. Surprisingly, after only a 10 s irradiation, a relatively larger amount of volatile nickel species could be produced in the HCOOH system. In order to avoid possible losses of volatile analyte species induced by any competitive photochemical (decomposition) reactions when longer irradiation times were attempted, a 6 m length of PTFE tubing ensured that the sample solution received a 4 min irradiation, and this was thus selected for further work.

Stability of resultant compounds

The effect of the length of the Tygon transfer line (placed between the gas–liquid separator and the F-AAS nebulizer) on the signal intensity from a 5 mg l^{-1} solution of Ni^{2+} was examined. No significant decrease in intensity was observed as the transport distance was increased (even up to 10 m), suggesting that, once formed and removed from the reactor, the volatile species is very stable and does not suffer detectable losses during the transport process. This conclusion is also supported by experiments wherein the volatile product was bubbled through solutions of 4 M HCl or NaOH, or when the transfer tube was immersed into an ice–salt trap (−2 °C), or hot water bath (40 °C). In all situations, no signal attenuation occurred.

Species identification

The tetracarbonyl is the only common volatile species of nickel, and its GC characteristics have been reported in an early study by Sunderman *et al.*[12] (electron capture detection using a 20 m Carbowax column), and electron-impact mass spectra have also been documented.[13,14] The volatile compounds formed in this study are inert to reaction in acidic and alkaline solutions and are stable at room temperature. These species can be trapped at low temperatures (partially, using a dry-ice–acetone bath at −78 °C; and completely, in a liquid nitrogen trap at −196 °C) and released on raising the temperature. This has permitted identification of their structures using GC–MS. The volatile species produced by subjecting a 1 l volume of sample containing 10 mg l^{-1} Ni^{2+}, 23 M HCOOH and 0.5 M HCOONa to UV irradiation were cryogenically trapped, as described earlier. Results from subsequent GC–MS measurements on this trapped product are shown in Fig. 6. Fragments containing nickel are easily

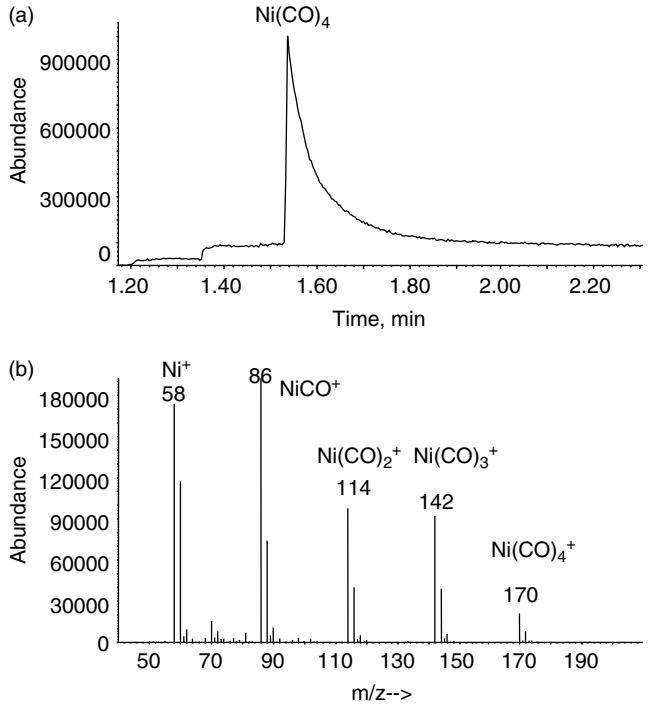

Figure 6. Electron-impact mass spectra arising from GC sampling of cryogenically trapped volatile nickel compounds produced by UV irradiation of solutions containing 10 mg l^{-1} Ni^{2+}, 23 M HCOOH and 0.5 M HCOONa: (a) the total ion chromatogram; (b) the mass spectrum taken at a retention time of 1.6 s.

recognized in the mass spectra as a result of their characteristic isotopic pattern (^{58}Ni (68.07%), ^{60}Ni (26.22%), ^{61}Ni (1.13%), ^{62}Ni (3.63%), and ^{64}Ni (0.925%)) arising from the five nickel isotopes present in the chromatographic peak. This isotopic pattern was evident in fragments for Ni^+ at m/z 58, $NiCO^+$ at m/z 86, $Ni(CO)_2^+$ at m/z 114, $Ni(CO)_3^+$ at m/z 142, and $Ni(CO)_4^+$ at m/z 170. No other chromatographic peaks indicative of the presence of additional species were detected. The resulting fragmentation patterns are in fair agreement with the reported mass spectrum of $Ni(CO)_4$,[13,14] which arises from stepwise loss of CO as the predominant fragmentation route. It may be concluded that the volatile nickel-containing species produced by UV photolysis of nickel chloride in HCOOH solutions is $Ni(CO)_4$. Identical results (a retention time of 1 min for the chromatographic peak and for the typical $Ni(CO)_4$ mass spectral patterns) were also obtained following irradiation of solutions containing 10 mg l^{-1} Ni^{2+} and 6.3 M CH_3COOH or 12 M CH_3CH_2COOH, but the relative ion intensities are comparatively lower. This is likely due to the low generation efficiency in these solutions, as suggested by the data in Fig. 2. Introduction of a sub-sample of the collected gas phase formed by treatment of CH_3CH_2COOH solutions during GC–ICP-MS resulted in the detection of only one nickel-containing peak, shown in Fig. 7.

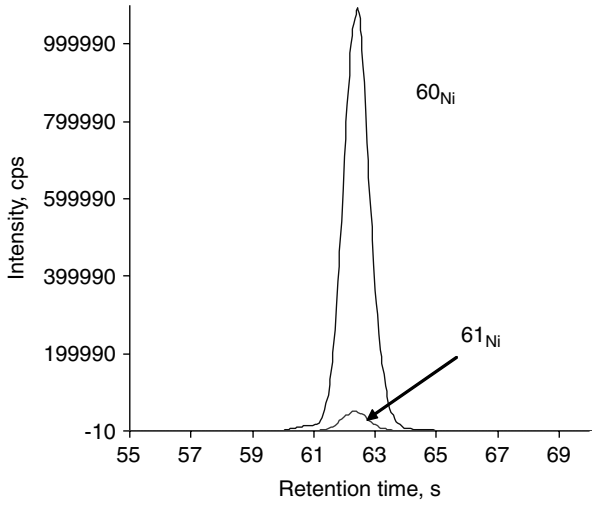

Figure 7. ICP-MS response from GC introduction of cryogenically trapped volatile nickel compounds produced by UV irradiation of solutions containing 10 mg l^{-1} Ni^{2+} in 13 M CH_3CH_2COOH.

Generation efficiency

The overall generation efficiency is defined as the convolution of the efficiency of species formation with those of its gas–liquid separation and transport to the detector. The overall efficiency was estimated from a comparison of the resulting F-AAS measurements made on solutions aspirated into the spectrometer before and after their irradiation. The results are presented in Table 1. Over the full range of nickel concentrations tested, more than 90% efficiency could be achieved. In order to deconvolute the efficiency components for gas–liquid separation and transport from that of photochemical generation, an irradiated 50 mg l^{-1} of Ni^{2+} sample solution was reprocessed through the reactor, once without additional irradiation (i.e. with the UV lamp off) and a second time with the lamp on. Without a second UV irradiation, approximately 2% of the total nickel was subsequently recovered by simple passage through the gas–liquid separation system, whereas about 7% of the nickel was detected as a volatile species following a second UV irradiation. It may be concluded that at least 2% of the volatile product remains in solution due to its solubility or because of inefficient phase separation, suggesting that the real photochemical generation or conversion efficiency is in excess of 95% in the HCOOH system. However, the efficiency of photochemical carbonylation was found to be concentration dependent, in that when higher concentrations of nickel were used, i.e. 500 mg l^{-1}, the generation efficiency appeared to decrease to less than 60%. No volatile product could be detected at concentrations above 1000 mg l^{-1}; a grey–black precipitate (probably finely divided active Ni^0) was produced instead.

Proposed mechanism

As discussed previously,[10] aliphatic organic acids may follow either of two different pathways during their

Table 1. $Ni(CO)_4$ generation efficiency

Nickel (mg l^{-1})		
Added	Unreacted[a]	Generation efficiency[b] (%)
1.0	0.10 ± 0.002	90 ± 2.0
5.0	0.28 ± 0.005	94 ± 1.6
10.0	0.49 ± 0.008	95 ± 1.6
50.0	3.60 ± 0.065	93 ± 1.8

[a] Residual Ni^{2+} in the reaction medium following UV irradiation.
[b] Estimated from solutions of 23 M HCOOH plus 0.5 M HCOONa following UV irradiation ($n = 5$).

anaerobic photolytic decomposition, which usually produces hydrocarbons, CO_2, and small amounts of CO and H_2, i.e.:

$$R{-}COOH \xrightarrow{h\nu} R^{\bullet} + {}^{\bullet}COOH \longrightarrow RH + CO_2 \quad (1)$$
$$(R = C_nH_{2n+1}, n = 0, 1, 2)$$

$$RCO{-}OH \xrightarrow{h\nu} RCO^{\bullet} + {}^{\bullet}OH \longrightarrow CO + ROH \quad (2)$$
$$(R = C_nH_{2n+1}, n = 0, 1, 2)$$

The resultant hydrogen and carboxyl radicals, which probably play a role in the reduction of Ni^{2+} to Ni^0, subsequently react with the CO produced in Eqn (2), resulting in the production of $Ni(CO)_4$:

$$4RCOOH + Ni^{2+} \xrightarrow{h\nu} Ni(CO)_4 + 4ROH \quad (3)$$
$$(R = C_nH_{2n+1}, n = 0, 1, 2)$$

In general, the reaction in Eqn (1) occurs more frequently than that in Eqn (2). In the case of HCOOH, the reaction in Eqn (1) occurs sixfold more frequently than that in Eqn (2).[15,16] In our earlier study of the UV-induced alkylation of inorganic selenium, we speculated that the reaction in Eqn (2) becomes less favorable with increasing carbon chain length because for $n = 1$ or 2 (acetic or propionic acid) the formation of selenium carbonyl was undetectable. This no longer appears to be the case for nickel. However, in consideration of the longer irradiation time required with the acetic or propionic acid systems, it is possible that another pathway exists for the formation of $Ni(CO)_4$. The organic acids are possibly decomposed into HCOOH by a photochemical process in the first step and then carbonylation of nickel may occur according to the reaction in Eqn (3). This may be the reason why a longer irradiation time is required compared with that for HCOOH. The details of the mechanism are not completely understood and must still be clarified. However, it is evident that, in the absence of UV light, there are no volatile nickel species formed (see Fig. 5).

CONCLUSIONS

This study is the first report of generation of $Ni(CO)_4$ from aqueous solutions of its inorganic salts using a direct photochemical approach, thereby offering an alternative route to its synthesis via green chemistry.

It is instructive to speculate about potential applications of this chemistry. It may be applied to extractive nickel metallurgy to produce pure nickel directly from solutions of acid leachates of its sulfide or oxide ores in the presence of LMW acids following UV irradiation.

$Ni(CO)_4$ is extremely poisonous (threshold limit is set at 0.001 ppm, compared with 10 ppm for hydrogen cyanide and 100 ppm CO).[17] Its carbonylation may occur in some nickel-contaminated foods, once LWM organic acids and UV light are abundantly available. This is the case when UV disinfection processes are employed to destroy yeasts, molds, bacteria, viruses and algae in the manufacturer of foods, pharmaceuticals and beverages in an environment where foods float in water past UV lamps for at least 15 to 20 min exposure.[18] A further concern is the disposal of nickel-containing materials to landfill. Formation of volatile nickel species, as well as molybdenum and tungsten carbonyls, has been reported in several investigations of municipal waste deposits.[19–22] As LMW acids are probably the end products of the degradation of the majority of organic compounds in nature, before being finally mineralized to CO_2, and H_2O, they are likely enriched in landfill sites or aquatic and terrestrial ecosystems. Exposure to UV radiation may result in the generation of toxic $Ni(CO)_4$ throughout the ecosystem.

Finally, application of this technique for analysis of trace concentrations of nickel remains to be explored.

Acknowledgements

X. G. gratefully acknowledges the financial support of a postdoctoral fellowship from NSERC.

REFERENCES

1. Mond L, Langer C, Quincke F. *J. Chem. Soc.* 1890; **57**: 749.
2. Ermler U, Grabarse W, Shima S, Goubeaud M, Thauer RK. *Science* 1997; **278**: 1457.
3. Zerner B. *Bioorg. Chem.* 1991; **19**: 116.
4. Volbeda A, Caron M-H, Piras C, Hatchikian EC, Frey M, Fontecilla CJC. *Nature* 1995; **373**: 580.
5. Youn H-D, Kim E-J, Hah YC, Kang S-O. *Biochem. J.* 1996; **318**: 889.
6. Dobbek H, Svetlitchnyi V, Gremer L, Huber R, Meyer O. *Science* 2001; **293**: 1281.
7. Menon S, Ragsdale SW. *Biochemistry* 1996; **35**: 12 119.
8. Ea AE. *Nickel Carbonyl*. The International Nickel Co.: New York, 1955.
9. Rochow EG. *Organometallic Chemistry*. Reinhold Publishing Corporation: USA, 1964.
10. Guo X, Sturgeon RE, Mester Z, Gardner JG. *Anal. Chem.* 2003; **75**: 2092–2099.
11. Guo X, Sturgeon RE, Mester Z, Gardner JG. *Appl. Organometal. Chem.* 2003; **17**: 575–579.
12. Sunderman Jr FW, Roszel NO, Clark RJ. *Arch. Environ. Health* 1968; **16**: 836.
13. Bidinosti DR, McIntyre NS. *Can. J. Chem.* 1967; **45**: 641.
14. Schildcrout SM, Pressley Jr GA, Stafford FE. *J. Am. Chem. Soc.* 1967; **89**: 1617.

15. Khriachtchev L, Maçôas E, Petterson M, Räänen M. *J. Am. Chem. Soc.* 2002; **124**: 10 994.
16. Langford SR, Batten AD, Kono M, Shfold MNR. *J. Chem. Soc.* 1997; **93**: 3757.
17. Nieboer E, Nriagu JO (eds). *Nickel and Human Health: Current Perspectives*. John Wiley: USA, 1992.
18. Tritsch GL. *Nutrition* 2000; **16**: 698.
19. Feldmann J, Cullen WR. *Environ. Sci. Technol.* 1997; **31**: 2125.
20. Feldmann J. *J. Environ. Monit.* 1999; **1**: 33.
21. Hetland S, Martinsen I, Radziuk B, Thomassen Y. *Anal. Sci.* 1991; **7**: 1029.
22. Sunderman FW. *Am. J. Clin. Pathol.* 1961; **35**: 203.

